DOI: 10.32615/bp.2019.015 BIOLOGIA PLANTARUM 63: 122-133, 2019

Overexpression of a gene *AhFBA* from *Arachis hypogaea* confers salinity stress tolerance in *Escherichia coli* and tobacco

Z.K. DU[1,2],·Y.F. HU[3],·and J.M. LI[1,2]*

Zhejiang Provincial Key Laboratory of Plant Evolution and Conservation, Taizhou University, Taizhou, Zhejiang 318000, P.R. China[1]
Institute of Ecology, Taizhou University, Taizhou, Zhejiang 318000, P.R. China[2]
College of Agronomy, Sichuan Agricultural University, Chengdu, Sichuan 611130, P.R. China[3]

Abstract

Fructose-1,6-bisphosphate aldolase (FBA), an essential enzyme involved in the glycolytic pathway, gluconeogenesis, and the Calvin cycle, plays significant roles in the regulation of plant growth, development, and stress responses. In this study, a novel gene, *AhFBA* (GenBank accession number KF470788), containing a 1077-bp open reading frame and encoding a protein of 358 amino acids, was isolated from *Arachis hypogaea* L. Bioinformatic analysis revealed that AhFBA belonged to class-I aldolases and preferentially localized in the cytoplasm. Real-time quantitative PCR analysis indicated that *AhFBA* had a higher expression in young fruits than in leaves and stems, and NaCl could trigger the highest expression of *AhFBA* in roots and leaves after 3-h and 6-h treatments. The salinity tolerance and survival of *Escherichia coli* transformed with *AhFBA* were notably enhanced compared with the control. Transgenic tobacco (*Nicotiana tabacum* L.) overexpressing the *AhFBA* gene exhibited a lower hydrogen peroxide content, electrolyte leakage, and malondialdehyde content and a higher photosynthetic efficiency, net photosynthetic rate, relative water content, and sucrose and proline content compared with control plants. Taken together, the results demonstrate that *AhFBA* functioned as a positive factor enhancing the tolerance of *E. coli* and *N. tabacum* to salinity stress, possibly by maintaining the osmotic balance and scavenging hydrogen peroxide.

Additional key words: fructose-1,6-bisphosphate aldolase, H_2O_2, net photosynthetic rate, *Nicotiana tabaccum*, peanut, proline, RWC.

Introduction

Fructose-1,6-bisphosphate aldolase (FBA, EC 4.1.2.13) catalyzes the reversible reaction of aldol fructose-1,6-bisphosphate (FBP) into triose dihydroxyacetone phosphate (DHAP) and glyceraldehyde-3-phosphate (G3P), which is a key enzyme for glycolysis, gluconeogenesis, and the Calvin cycle (Haake *et al.* 1998). The FBAs can be divided into two groups according to the catalytic mechanism employed. Class I FBAs are mainly found in plants, animals, and green algae (only occasionally in bacteria), forming a Schiff-base using the ε-amino group of a conserved lysine residue in the active center of the enzyme with the C-2 carbonyl group of the substrate (FBP or DHAP) (Shams *et al.* 2014). Class I FBAs can form tetramers in eukaryotes, and they are not inhibited by a chelating agent EDTA. However, class II FBAs are mainly found in bacteria and fungi, utilizing a divalent metal ion (usually Zn^{2+} or Fe^{2+}) at the active site as an electrophile to stabilize the carbanion formed on the third carbon of the substrate. Furthermore, class II FBAs are dimers and can be inhibited by EDTA (Gross *et al.* 1999).

Submitted 2 March 2018, *last revision* 21 June 2018, *accepted* 7 August 2018.
Abbreviations: DHAP - dihydroxyacetone phosphate; EC - electrical conductivity; FBA - fructose-1,6-bisphosphate aldolase; FBP - fructose-1,6-bisphosphate; G3P - glyceraldehyde-3-phosphate; IPTG - isopropyl β-D-1-thiogalactopyranoside; LB - Luria-Bertani; MDA - malondialdehyde; ORF - open reading frame; qPCR - quantitative polymerase chain reaction; P_N - net photosynthetic rate; ROS - reactive oxygen species; RWC - relative water content.
Acknowledgments: This study was funded by the Public Welfare Project of Science Technology Department of Zhejiang Province (LGN18C160002), the National Natural Science Foundation of China (31270461; 31571757), and the Science and Technology Program of Yuhuan City, China (201603).
* Corresponding author; fax: (+86) 576 88660892; e-mail: lijm@tzc.edu.cn

The FBAs in green plants have two isozymes, a cytosolic FBA (cFBA) and a chloroplast/plastid FBA (cpFBA) (Lebherz *et al.* 1984). The cFBA is a vital enzyme that catalyzes the reversible cleavage of FBP into DHAP and GAP in the glycolytic and gluconeogenesis pathways in the cytoplasm, which plays an important role in plant growth and tolerance to environmental stresses. Antisense inhibition of *OscFBA* expression in rice decreases the amount of FBA in roots and suppresses the growth of roots compared with wild-type plants (Konishi *et al.* 2004). Likewise, cFBA is more active in elongating tissues of *Phyllostachys pubescens* than in those that have completed elongation (Lao *et al.* 2013). Moreover, overexpression of *cSlFBA* in tomato enhances the seed germination rate under low and high temperature stresses (Cai *et al.* 2016). In contrast, cpFBA is an essential enzyme in the Calvin cycle, where it catalyzes the reversible reaction of sedoheptulose-1,7-bisphosphate into DHAP and erythrose-4-phosphate in the chloroplast, in addition to the reversible condensation of DHAP and G3P to FBP (Flechner *et al.* 1999). Overexpression of the *Arabidopsis thaliana* cpFBA gene in tobacco significantly enhances the photosynthesis CO_2 fixation rate and growth of transgenic plants, particularly at a high CO_2 concentration (Uematsu *et al.* 2012).

Increasing evidence has suggested that *FBA* genes participate in many physiological and biochemical reactions in plants, including chloroplast development (Zhang *et al.* 2016), CO_2 fixation (Uematsu et al. 2012), plant growth (Lao *et al*. 2013), and oil yield (Zeng *et al.* 2014), as well as in plant resistance to biotic (Mohapatra and Mittra 2016) and abiotic stresses such as drought (Cheng *et al.* 2016), chilling (Purev *et al.* 2008), salt (Zeng *et al.* 2015), and cadmium (Singh *et al.* 2015). A large number of *FBA* genes have been identified in many plant species, *e.g*., in maize (Dennis *et al.* 1988), rice (Kagaya *et al*. 1995), *Camellia oleifera* (Zeng et al. 2015), tomato (Cai et al. 2016), and wheat (Lv *et al.* 2017).

Although studies on *FBA* genes from other species have been widely reported, little is known about this gene in peanut. Peanut, as a main source of vegetable oil and plant protein, is widely planted in tropical and subtropical regions, of which at least 15 % are affected by salt stress (Kavas *et al.* 2015). Therefore, to achieve a better understanding of the molecular mechanism of salt tolerance in peanut, it is necessary to identify the responses of its genes to salinity stress. A recent report showed that the *FBA* gene of *A. hypogaea* is responsive to salinity stress (Sui *et al.* 2016); however, the functions of this gene under salt stress are still not clear. Therefore, a novel cytoplasmic gene *AhFBA* was isolated from peanut and used to generate *AhFBA*-overexpressing *Escherichia coli* and tobacco lines to determine the physiological functions of *AhFBA*.

Materials and methods

Plants and growth conditions: Peanut (*Arachis hypogaea* L. cv. Xiaojingsheng) seeds purchased from the Xinchang Seeds Company were sterilized by soaking in a 2 % (m/v) $NaClO_4$ for 10 min and grown in a growth chamber at a temperature of 25 °C, a relative humidity of 75 %, a 16-h photoperiod, and an irradiance of 400 μmol m^{-2} s^{-1} until the fourth leaf was fully expanded. Seeds of *Nicotiana tabaccum* L. cv. Yunan 85 were surface-sterilized with 70 % (v/v) ethanol for 2 min and 1 % (m/v) $NaClO_4$ for 10 min followed by six washes with sterile water. They were then sown in plastic trays filled with a mixture of *Perlite* and *Vermiculite* (1:1, v/v) for germination in the above mentioned growth chamber.

Isolation of RNA and cDNA synthesis: Total RNA was extracted from peanut leaf samples with a *TRIzol* reagent (*Promega*, Madison, USA) according to the manufacturer's instructions. An RNA quality assessment was performed by agarose gel electrophoresis, and the concentration was measured with a *NanoDrop™ ND-1000* (*Nanodrop Technologies*, Wilmington, DE, USA) spectrophotometer. The first-strand cDNA was synthesized from total RNA using a *PrimeScript™* 1st strand synthesis kit (*TaKaRa*, Dalian, China) according to the manufacturer's instructions.

***In silico* cloning the *AhFBA* gene from *Arachis hypogaea*:** The protein sequence of FBA (*GenBank* accession number AY492006.1) from *Glycine max* was used as a query probe for a *tBLASTn* search against the *Arachis hypogaea EST* database at the National Center for Biotechnology Information (*NCBI*) website. A total of 15 peanut ESTs (GO257556.1, FS966168.1, FS971324.1, FS961748.1, FS982176.1, FS965569.1, FS979209.1, FS969910.1, ES705591.1, FS974377.1, FS978710.1, ES710499.1, FS973585.1, FS766474.1, and FS979097.1) sharing a high similarity with the reference sequence were subjected to contig assembly using the *SeqMan* program, and an *EST* contig with a length of 1 376 bp was obtained. The putative full-length cDNA of *AhFBA* was analyzed using *ORF Finder*, and one open reading frame (ORF) with a length of 1 077 bp was identified. Primers AhFBA-C-F and AhFBA-C-R (Table 1 Suppl.) were then designed to amplify the putative ORF sequence using cDNA as a template.

Experimental verification and sequence analyses of *AhFBA*: Reaction mixtures for PCR (20 mm^3) contained 2.0 mm^3 of template cDNA (20 ng), 2.5 mm^3 of dNTP mixture (2.5 mM dATP, 2.5 mM dGTP, 2.5 mM dCTP, and 2.5 mM dTTP), 2.0 mm^3 of 10× PCR buffer, 0.1 mm^3 of each primer (10 μM), 0.1 mm^3 of KOD plus DNA

polymerase (*Toyobo*, Shanghai, China), and 13.2 mm^3 of double distilled H_2O. The PCR reaction program was as follows: an initial denaturation at 94 ºC for 5 min followed by 30 cycles of denaturation at 94 °C for 40 s, annealing at 55 °C for 40 s, and extension at 72 °C for 1.5 min, and a final extension reaction at 72 °C for 10 min. The PCR products were detected on a 1 % (m/v) agarose gel, and then the single specific band was purified using a DNA gel extraction kit (*Beyotime*, Haimen, China) and ligated to the pUCm-T vector (*Beyotime*) to construct a recombinant vector pUCm-T-AhFBA. Positive clones were sequenced with an *ABI 3130XL* genetic analyzer (*Applied Biosystems*, Foster City, USA).

Bioinformatics analyses: Amino acid sequence alignment analysis was performed with *DNAMAN 7.0* (*Lynnon Biosoft*, Quebec, Canada). The protein active site was identified by searching the *Motif Scan* database (http://myhits.isb-sib.ch/cgi-bin/motif_scan). Signal peptides were predicted using *SignalP 4.1* (http:// www.cbs.dtu.dk/services/SignalP-4.1/). A phylo-genetic tree of FBA proteins in different species was constructed with *MEGA 5.05* (Tempe, AZ, USA) using the unweighted pair-group method with the arithmetic mean. The AhFBA protein sequence (GenBank accession number AGV08373.1) was submitted to *SwissModel* (http:// swissmodel.expasy.org/) for structural modeling. The modeled tertiary and quaternary structures were analyzed in *Swiss-PdbViewer*.

Gene expression profile analysis by real-time quantitative PCR: A pair of specific primers, AhFBA-SYBR-F and AhFBA-SYBR-R (Table 1 Suppl.), avoiding the conserved region, were designed for real-time quantitative PCR (qPCR) to amplify a product of 100 - 200 bp from *AhFBA* cDNA of roots, leves, flowers, gynophores, and young fruits. The 18S rRNA gene was used as an internal control gene. Cycle threshold (Ct) values were determined for each sample, and the relative gene expression levels of control gene expression were calculated using the $2^{-\Delta\Delta Ct}$ method (Schmittgen and Livak 2008).

Expression of a recombinant protein AhFBA in *E. coli*: The PCR products of the *AhFBA* gene amplified with primers AhFBA-E-F and AhFBA-E-R (Table 1 Suppl.) were purified with a DNA gel extraction kit (*Beyotime*) and digested with *Bam*HI and *Sal*I followed by ligation into pET28a (+) digested with the same restriction endonucleases to construct a recombinant plasmid pET28a-AhFBA. The plasmid pET28a-AhFBA was then transformed into *E. coli* strain BL21(DE3), and positive clones were verified by sequencing. The positive recombinant cells were cultivated at 37 ºC in a Luria-Bertani (LB) medium containing 50 $mg \cdot dm^{-3}$ kanamycin until the cells were grown to the mid-log phase ($A_{600} \approx 0.5$), followed by induction with 0.1 mM isopropyl-β-D-1-thiogalacto-pyranoside (IPTG) at 37 ºC on a shaking incubator at 120 rpm for 1, 2, 3, 4, and 5 h. The soluble protein fractions were separated on a 12 % (m/v) SDS-PAGE gel and stained with Coomassie Brilliant Blue G-250.

Assay for salt tolerance of *E. coli* BL21(DE3) transformed with pET28a-AhFBA: Single colonies of BL21(DE3) cells harboring either pET28a or pET28a-AhFBA were inoculated on a LB liquid medium containing 50 $mg \cdot dm^{-3}$ kanamycin. Induction of AhFBA protein was performed according to the procedure described above using 0.1 mM IPTG for 2 h. The cultures were serially diluted 10-fold, and then 5-mm^3 dilutions of each sample were spotted onto LB medium plates containing 0.1 mM IPTG and 200 mM NaCl. The bacteria were grown in the dark at 37 °C for 12 h and observed with a digital camera. In other experiment, cultures of BL21(DE3) (harboring pET28a or pET28a-AhFBA) were inoculated on 50 cm^3 of a LB medium supplemented with 50 $mg \cdot dm^{-3}$ kanamycin and 200 mM NaCl. Absorbance at 600 nm of the bacterial cultures were adjusted to approximately 0.2 and induced by 0.1 mM IPTG at 37 ºC. Samples of 1 cm^3 were harvested every 60 min, and absorbance at 600 nm was measured using a *T6* spectrophotometer (*Puxi*, Shanghai, China).

Subcellular localization of AhFBA protein: The ORF of *AhFBA* was amplified using specific primers AhFBA-E-F and AhFBA-E-R (Table 1 Suppl.), and then the purified PCR product was digested with *Bam*HI and *Sal*I followed by insertion into the multiple cloning site of the expression vector pCAMBIA1300-GFP to generate a recombinant vector pCAMBIA1300-AhFBA-GFP. The vector pCAMBIA1300-AhFBA-GFP was introduced into *Nicotiana tabacum* cv. Yunyan 85 cells *via Agrobacterium tumefaciens* LBA4404 (Zhang *et al.* 2015), and the AhFBA-GFP fusion protein was induced under the control of the CaMV 35S promoter from the cauliflower mosaic virus. The green fluorescence protein signal was observed with a confocal laser scanning fluorescence microscope (*Olympus*, Tokyo, Japan).

Transformation of AhFBA in tobacco: LBA4404 harboring the recombinant plasmid pCAMBIA1300-AhFBA-GFP was introduced into *N. tabacum* cv. Yunyan 85 leaves by the leaf-disc method. Putative transgenic seedlings were screened on Murashige-Skoog (MS) medium plates containing 100 $mg \cdot dm^{-3}$ kanamycin and confirmed by PCR analysis using primers AhFBA-E-F and AhFBA-E-R (Table 1 Suppl.). The seeds of all transgenic lines were harvested and germinated on an MS solid medium containing 100 $mg \cdot dm^{-3}$ kanamycin to select transgenic lines carrying a single copy of the integrated *AhFBA* gene, and transgenic offspring showing the expected segregation ratio of 3:1 were chosen for the production of T_1 progeny.

Salinity tolerance of transgenic tobacco: Seeds from T_1 progeny transgenic lines were surface-sterilized with 70 % (v/v) ethanol for 2 min and 1 % (m/v) $NaClO_4$ for 10 min followed by six washes with sterile water. They were then sown in plastic trays filled with a mixture of *Perlite* and *Vermiculite* (1:1, v/v) for germination in the above mentioned growth chamber. Two-week-old control (transformed with the empty vector pCAMBIA1300-GFP) and T_1 transgenic seedlings were transplanted into pots containing soil, humus, and sand (2:1:1, v/v/v) and then cultured for three weeks. To evaluate salt tolerance, transgenic and control plants were irrigated with 500 mM NaCl every third day for 6 d. After NaCl treatment, the third and fourth leaves from the shoot apex were used for measurements of gas exchange parameters and physiological analyses.

Measurements of physiological parameters: Chlorophyll fluorescence was measured at 25 °C using a *OS30P* portable modulated fluorometer (*Opti-Sciences*, Hudson, NH, USA) as described by Toscano *et al.* (2016). Net photosynthesis rate (P_N) was measured using a *LI-6400* portable photosynthesis system (*Li-Cor*, Lincoln, USA). The parameters in the measuring chamber were: a CO_2 concentration of 400 μmol·mol^{-1}, photosynthetically active radiation (PAR) of 1500 μmol·m^{-2}·s^{-1}, a temperature of 25 °C and a relative humidity of 65 %.

Determination of the relative water content (RWC) and proline content were performed according to Patel *et al.* (2015) by gravimetric method and acidic ninhydrin method, respectively. Content of H_2O_2 was assessed with potassium iodide (KI) reagent following Chen *et al.* (2016). Content of MDA and electrolyte leakage were determined according to Park *et al*. (2017) by thio-barbituric acid (TBA) method and electrical conductivity method, respectively. Sucrose content was measured by adding hydroxyphenol solution and recording absorbance at 480 nm described by Shi *et al.* (2012).

Statistical analysis: Statistical analyses were performed using three independent biological replicates. The values provided in the figures and tables are presented as means ± SEs. Data were analyzed by one-way analysis of variance (*ANOVA*) and the Duncan multiple comparison test using the *SPSS 18.0* software (*SPSS*, Chicago, IL, USA). Different lowercase letters on the histograms indicate that the means were significantly different at $P < 0.05$.

Results

Two primers were employed to amplify the ORF of *AhFBA,* and one approximately 1 000-bp real-time PCR product was harvested (Fig. 1 Suppl.) and sequenced in both directions. Sequence comparisons between the assembled contig and the PCR product showed that the two sequences were the same, supporting the credibility of the *in silico* cloning results. The *AhFBA* cDNA generated by PCR contained an ORF of 1 077 bp encoding 358 amino acid residues, and the sequence was submitted to the *GenBank* (accession number KF470788.1). The deduced AhFBA protein had a predicted molecular mass of 38.38 kDa and a theoretical isoelectric point of 6.73. Signal peptide prediction by *SignalP* revealed no signal peptide in the protein of AhFBA, implying that AhFBA might not be a secreted protein.

Multiple sequence alignment of the amino acid sequences showed that the sequence of AhFBA protein was highly homologous to that of other plant FBA sequences, sharing 92.18, 91.34, 91.06, 89.66, 87.43, 85.75, and 84.36 % amino acid sequence similarity with *Medicago truncatula*, *Phaseolus vulgaris*, *Glycine soja*, *Citrus clementina*, *Arabidopsis lyrata*, *Solanum tuberosum*, and *Triticum aestivum*, respectively. Furthermore, it also contained one conserved domain, VLLEGTLLKPN (217-227), the class-I active site of FBA. This conserved motif could form a Schiff-base between the ε-amino group of lysine in the active site and the carbonyl group of the substrate (Fig. 2 Suppl.).

To study the phylogenetic relationship of AhFBA proteins from a variety of plants, a phylogenetic tree was constructed and revealed three major clades, dicotyledons, monocotyledons, and green algae (Fig. 3 Suppl.). AhFBA was grouped into one cluster of dicotyledons together with FBAs from other legume plants including *M. truncatula*, *P. vulgaris* and *G. soja* (Fig. 3 Suppl.).

The tertiary and quaternary structures of the AhFBA protein were predicted with *SwissModel*. The results showed that the monomer of AhFBA consisted of 12 α-helix and 12 β-sheet secondary structures (Fig. 1*A*). In addition, AhFBA could be classified as a class I subfamily because it could form homotetramers containing interfaces A and B, similar to other class I subfamily FBAs. In AhFBA, each interface B had six hydrogen bonds consisting of the carboxylate O atoms of Asp124 and the backbone amides of three consecutive residues (G122-L123-D124) of the homologous subunit. Compared with interface B, which displayed loop-loop interactions formed by hydrogen bonds, interface A was composed of helix-packing interactions (Fig. 1*B*). Although the peripheral amino acid residues of the active site differed among the FBAs, the catalytic residues in the active site interior were highly conserved. The catalytic residues in AhFBA had also highly conserved catalytic residues, which included D30-K103-K142-R144-E183-E185-K225-S266-R298 (Fig. 1*C*).

To analyze the expression patterns of *AhFBA*, mRNA isolated from different tissues of peanut was used as the template for real-time qPCR. Although the *AhFBA* gene

transcription was detected in all tested tissues, the expressions were significantly different ($P < 0.05$). The transcript abundances of *AhFBA* in leaves were lowest, and those in young fruits, gynophores, and roots were approximately 4.0-, 5.3- and 8.3-fold higher, respectively (Fig. 2*A*). To characterize the expression pattern of the *AhFBA* gene under NaCl stress for various times, real-time qPCR was also employed. As shown in Fig. 2*B*, the transcription of *AhFBA* was upregulated and showed approximately 7.4- and 5.8-fold increases at 3 and 6 h after the treatment with 400 mM NaCl in roots and leaves, respectively. These results suggest that the *AhFBA* gene could be induced by NaCl treatment.

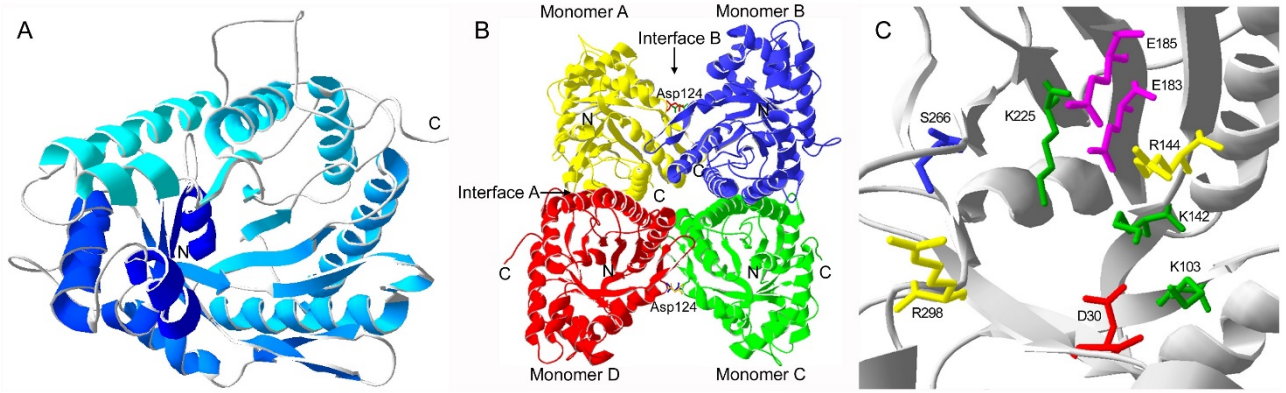

Fig. 1. Predicted tertiary and quaternary structures of the AhFBA protein. *A* - Monomer AhFBA; *B* - tetrameric AhFBA; *C* - amino acid residues in the active site of AhFBA. For *A*,*B*, carboxyl-termini and amino-termini are denoted by *C* and *N*, respectively. For *B*, each monomer in the tetramer is labeled with one color, and the *arrows* indicate interfaces A and B. The Asp124 forms hydrogen bonds with amino acid residues in the adjacent monomer on interface B.

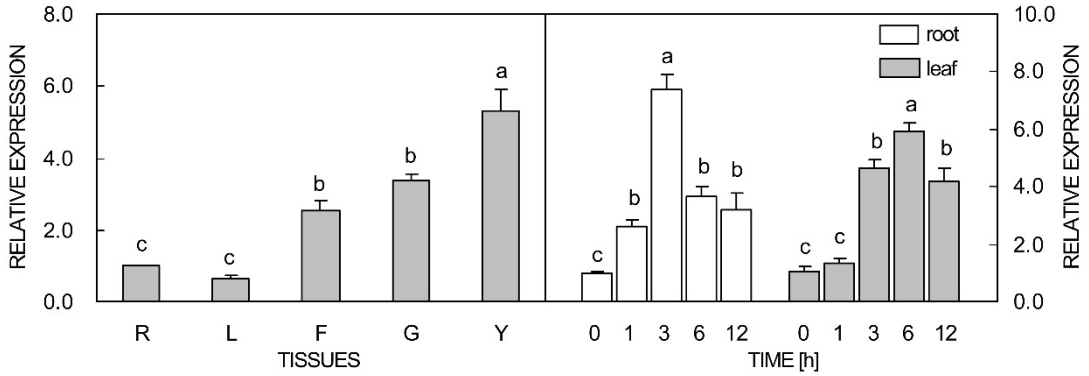

Fig. 2. Relative expressions of *AhFBA* in different tissues of *Arachis hypogaea* measured by real-time quantitative PCR. Expression patterns of *AhFBA* in roots (R), leaves (L), flowers (F), gynophores (G), and young fruits (Y) of control plants (*on the left*). Expression patterns of *AhFBA* roots and leaves under 400 mM NaCl for 1 to 12 h (*on the right*). Data are the means ± SEs from three biological replicates. Different lowercase letters indicate significant differences ($P < 0.05$).

The recombinant AhFBA protein was strongly induced by IPTG in *E. coli* strain BL21(DE3) when the coding sequence of *AhFBA* was integrated into the multiple cloning site of the expression vector pET28a under control of the T7 promoter. A distinct protein band with a molecular mass between 31.0 and 43.0 kDa, consistent with the predicted value, was detected on the SDS-PAGE gel of total proteins following induction for 1 to 5 h with 0.1 mM IPTG, compared to the BL21(DE3) strain containing pET28a incubated with IPTG (Fig. 3*A*).

To assess whether AhFBA is involved in protecting against NaCl stress, a spotting assay was employed to investigate the growth response of *E. coli* cultures (with and without expression of recombinant AhFBA) under NaCl stress. The plate spotting experiments revealed that both pET28a-AhFBA and pET28a (control) vector-transformed *E. coli* BL21(DE3) cells had similar growth performances (Fig. 3*B*). However, pET28a-AhFBA-transformed cells showed a significant growth advantage (a larger size and greater number of colonies) compared with control cells when subjected to the addition of 200 mM NaCl to the LB medium (Fig. 3*C*). In the liquid medium, pET28a-AhFBA-bearing *E. coli* cells entered a logarithmic phase earlier than pET28a-bearing *E. coli* cells, but absorbance at 600 nm did not differ between them after cultivation for 11 h in the absence of NaCl

(Fig. 3*D*). Addition of 200 mM NaCl to the LB medium inhibited the growth of both cell strains, but *E. coli* cells harboring pET28a-AhFBA showed a significantly diminished reduction of the growth rate compared with *E. coli* cells harboring pET28a (Fig. 3*E*).

To explore how the function of *AhFBA* is related to NaCl stress adjustment in plants, the expression vector pCAMBIA1300-GFP (Fig. 4*A*) containing the coding sequence of *AhFBA* was introduced into tobacco (*N. tabacum* cv. Yunyan 85) *via* the *Agrobacterium*-mediated leaf disc transformation method to generate transgenic tobacco plants. The empty pCAMBIA1300-GFP was transformed into tobacco using the same method as a control. Positive transgenic lines were screened based on kanamycin resistance and confirmed by PCR detection using leaf genomic DNA as a template. The PCR analysis revealed a specific band of approximately 1 000 bp in all seven transgenic lines (Fig. 4*B*) implying that the coding sequence of *AhFBA* was successfully transformed into tobacco. Furthermore, the transcriptional profiles of *AhFBA* were detected by real-time qPCR in T_1 transgenic lines. As shown in Fig. 4C, the expression of *AhFBA* varied in seven transgenic lines, whereas the expression was not detected in control plants. Three independent transgenic lines (L_2, L_5, and L_6) with the highest expressions were selected for further study.

To explore the subcellular localization of AhFBA, the recombinant vectors pCAMBIA1300-AhFBA-GFP and pCAMBIA1300-GFP (as a control) were transiently expressed in tobacco leaves (mediated by *Agrobacterium* strain LBA 4404). Confocal microscopy analysis indicated that 35S-GFP showed fluorescence signal throughout the whole epidermal cell (Fig. 5*A*-*C*), whereas the recombinant protein AhFBA-GFP had a strong

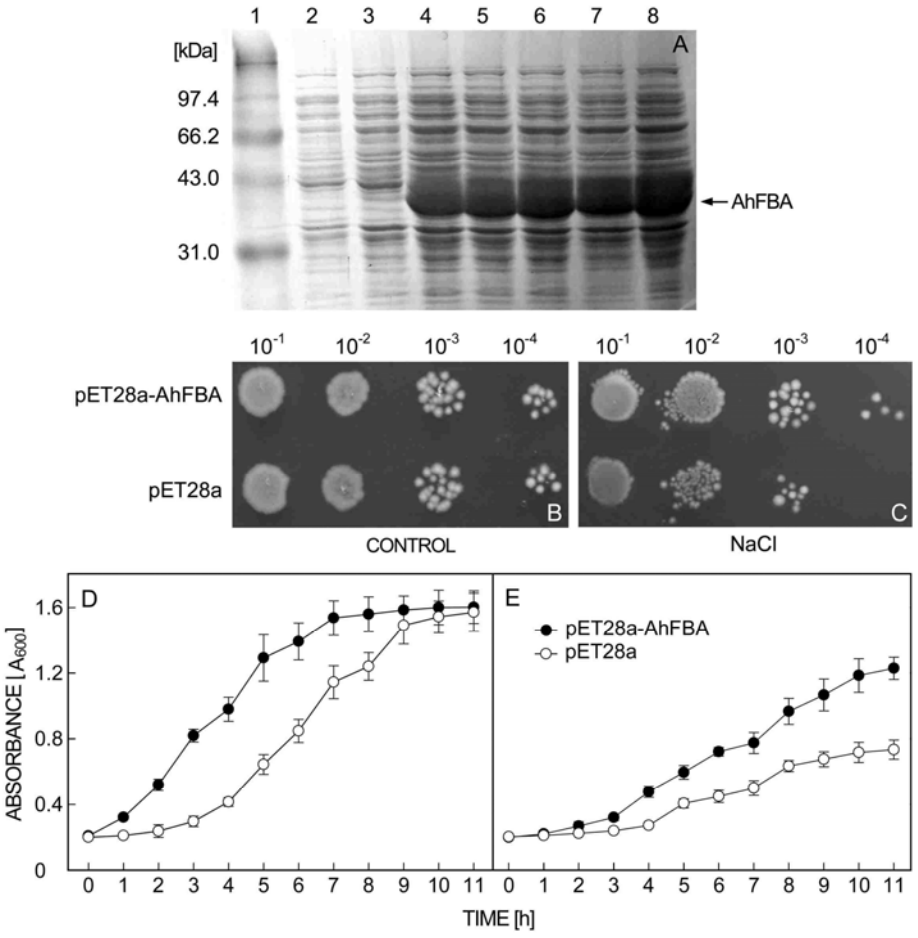

Fig. 3. Analysis by SDS-PAGE of the recombinant protein AhFBA expressed in *Escherichia coli* strain BL21(DE3) and the role of protein AhFBA in NaCl stress tolerance of *E. coli*. *A* - *lane* 1 - protein marker; *lane* 2 - proteins from BL21(DE3) cells harboring a plasmid pET28a induced at 37 °C with 0.1 mM IPTG for 3 h, *lanes* 3, 4, 5, 6, 7 and 8 - proteins from BL21(DE3) cells carrying recombinant plasmid pET28a-AhFBA induced at 37 °C with 0.1 mM IPTG for 0, 1, 2, 3, 4, and 5 h. Proteins were visualized with Coomassie brilliant blue G-250. The *arrow* indicates the target protein with a molecular mass of approximately 38 kDa. Cultures of BL21(DE3) (harbouring pET28a-AhFBA or pET28a) were serially diluted and spotted on a solid LB medium without (*B*) or with (*C*) addition of 200 mM NaCl. Growth curves of *E. coli* transformed either with pET28a-AhFBA or with pET28a in a liquid LB medium without (*D*) and with (*E*) 200 mM NaCl. Means ± SEs, $n = 3$.

cytoplasmic signal in the cells (Fig. 5*D-F*).

To determine whether the overexpression of protein AhFBA could enhance salinity tolerance, five-week-old tobacco plants were irrigated with 500 mM NaCl solution every 3rd day, and the growth performance of positive transgenic plants was compared with control plants (Fig. 6). The results revealed no obvious phenotypic differences among control and transgenic tobacco plants grown under normal conditions. However, the control plants showed wilted leaves after 4 d of 500 mM NaCl treatment, whereas the transgenic L_2, L_5, and L_6 all maintained healthy leaves. Chlorophyll loss and withered and yellow leaves were observed in control plants with the prolongation of salt stress to 7 d, but transgenic lines displayed good growth and less bleaching leaves. The phenotypic characteristics suggest that overexpression of *AhFBA* enhanced the tolerance of tobacco to salinity.

To explore the effects of *AhFBA* overexpression on the salinity tolerance of tobacco, some physiological parameters were measured in control and transgenic plants

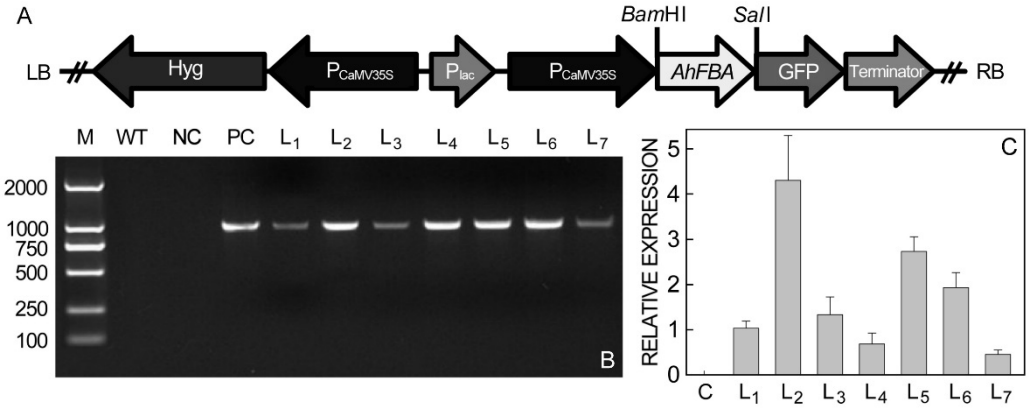

Fig. 4. Generation and detection of transgenic tobacco plants expressing the *AhFBA* gene. *A* A schematic diagram of the construction of the recombinant plasmid pCAMBIA1300-AhFBA-GFP. The *AhFBA* coding sequence was ligated into pCAMBIA1300-GFP under the control of the promoter CaMV 35S. LB - left border, RB - right border. *B* The PCR amplification of the genomic DNA confirmed the introduction of the *AhFBA* gene into transgenic tobacco lines. M - DL2000 DNA marker, WT - wild-type, NC - negative control, PC - positive control, L_1 to L_7 - independent transgenic tobacco T_1 lines overexpressing *AhFBA*. *C* - The *AhFBA* transcript abundance in control and transgenic plants. C - control; L_1 to L_7, seven transgenic lines.

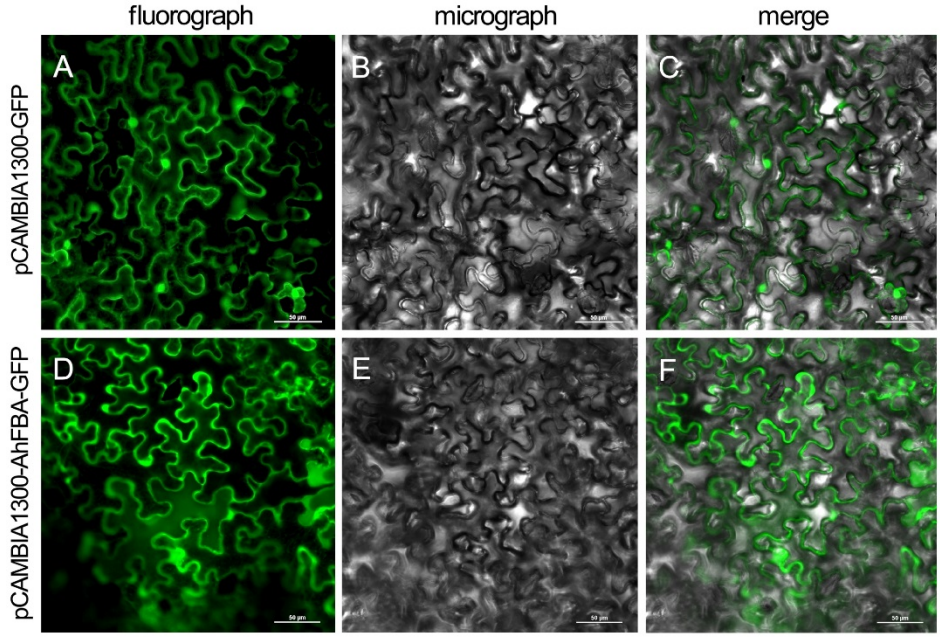

Fig. 5. Subcellular localization of AhFBA in *Nicotiana tabacum* cv. Yunyan 85. The coding sequence of *AhFBA* was cloned into the pCAMBIA1300-GFP vector under the control of the CaMV 35S promoter and transformed into leaves of *N. tabacum*. Images were observed using a confocal laser scanning microscope to observe green fluorescence in dark field 48 h after agroinfiltration (*A*,*D*), cell morphology in bright field (*B*,*E*), and their combination (*C*,*F*). The empty vector (pCAMBIA1300-GFP) was used as a control.

(L_2, L_5, and L_6) grown under normal and salt-stressed conditions.

In the absence of NaCl (0 d), there were no significant differences in photosynthetic efficiency (the variable to maximum chlorophyll fluorescence ratio, F_v/F_m) among control and transgenic plants (Fig. 7*A*). When subjected to 500 mM NaCl for 4 and 7 d, the value of F_v/F_m were significantly lower in control plants compared with transgenic lines. The P_N was significantly higher in transgenic lines L_2 and L_5 than in control plants when exposed to NaCl treatment for 4 and 7 d (Fig. 7*B*). Increased generation of H_2O_2 in plants exposed to stresses usually causes a disruption of membrane integrity, which can be also estimated by measuring electrolyte leakage and MDA content in the plants. The results indicate no significant differences in H_2O_2 content, electrolyte leakage, and MDA content between control and transgenic plants without salt stress; however, an increase in H_2O_2 content, electrolyte leakage, and MDA content were observed in control plants exposed to 500 mM NaCl. Also, RWC was lower in control plants compared with transgenic lines following the application of salt stress (Fig. 7*C-F*). Sucrose and proline may function as an osmoprotectants maintaining pressure potential, and they also stabilize cellular membranes. Although there were no significant differences in sucrose content between control and transgenic plants under control conditions, all transgenic lines accumulated a significantly higher amount of sucrose than control plants under salinity (Fig. 7*G*). Similarly, proline content was significantly higher in transgenic lines than in control plants at the fourth day of salinity treatment (Fig. 7*H*).

Fig. 6. Growth performances of control (WT) and *AhFBA* overexpressing T_1 transgenic line (L_2, L_5, and L_6) tobacco plants irrigated with a 500 mM NaCl solution for 4 and 7 d.

Discussion

The FBA is a multiple functional protein, which participates in a wide range of biological processes. It is well known that FBA catalyzes the cleavage of FBP into G3P and DHAP and further a reversible aldol condenzation, and it is a vital enzyme in glycolysis, gluconeogenesis, and the Calvin cycle (Haake *et al*. 1998). Recently, FBA has been shown to participate in other functions in cells, such as the binding of class I cFBA in *Medicago sativa* to the transcription factor NMH7 (Páez-Valencia *et al.* 2008) and the physical interaction of yeast FBA1 with the RNA polymerase III (Pol III) complex (Cieśla *et al*. 2014).

Although *FBA* genes have been isolated and studied in numerous plant species, few studies have examined the *AhFBA* gene in peanut. In this research, the ORF of the *AhFBA* gene in *A. hypogaea* was cloned and characterized, and its amino acid sequence showed a high homology with those from *M. truncatula*, *P. vulgaris*, and *C. clementina*. Sequence alignment indicates that *AhFBA* was a class-I aldolase. Moreover, subcellular localization demonstrates that *AhFBA* was located in the cytoplasm. In the present study, overexpression of the protein AhFBA in *E. coli* and tobacco enhanced salinity tolerance compared with controls in agreement with previously reported studies (Fan *et al.* 2009, Zeng *et al.* 2015, Cai *et al.* 2016). Thus, the *AhFBA* gene could play a positive role in responses to NaCl stress.

Two isoenzymes of FBA in green plants are cpFBA and cFBA. The former is a significant enzyme in the Calvin cycle in the chloroplast, and the latter is a vital enzyme in glycolytic processes and gluconeogenesis in the cytoplasm (Lebherz et al. 1984). Overexpression of the *Solanum lycopersicum* cFBA gene in tomato increases the activities of the main enzymes involved in the Calvin cycle and also P_N (Cai *et al.* 2016); however, no significant increase in P_N was observed in transgenic tobacco lines without salinity stress compared with twild type plants (Fig. 7*B*). Similar results have been obtained by Uematsu *et al*. (2012), who observed that overexpression of the *Arabidopsis thaliana cpFBA* gene in tobacco does not enhance photosynthesis in the transgenic plants, particularly at an ambient CO_2 concentration. Since the photosynthesis rate is limited by the activity of ribulose-1,5-bisphosphate carboxylase/oxygenase at relatively low CO_2 concentrations, our results suggest that overexpression of the *cFBA* gene in tobacco might not increase the activity of ribulose-1,5-bisphosphate carboxylase/oxygenase, and that a native plastid FBA

activity is sufficient for photosynthesis at ambient CO_2 concentrations without environmental stress. Although P_N of transgenic tobacco lines was notably higher than in control plants under salinity stress for 4 and 7 d, the main explanation might be that photosystem II was less damaged by NaCl in transgenic plants compared with control plants (Fig. 7*A*).

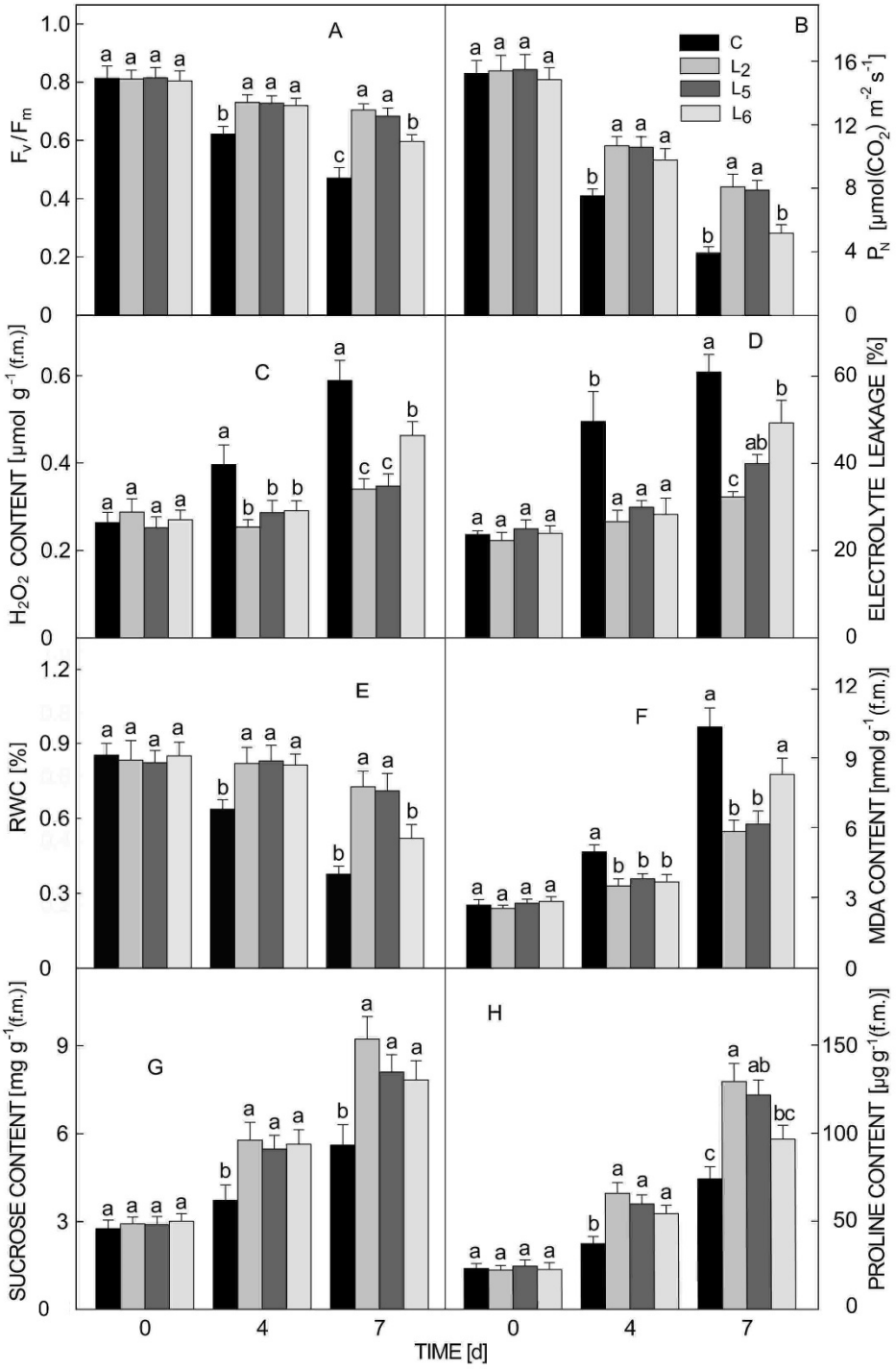

Fig. 7. Physiological analysis of control and transgenic plants (L_2, L_5, and L_5) grown under 500 mM NaCl for 0 to 7 d. *A* - photosynthetic efficiency, F_v/F_m; *B* - net photosynthetic rate, P_N; *C* - H_2O_2 content; *D* - electrolyte leakage; *E* - relative water content, RWC; *F* - malondialdehyde (MDA) content; *G* - sucrose content; H - proline content. Means ± SEs from three biological replicates. Different lowercase letters indicate significant differences ($P < 0.05$).

A major threat to agriculture, especially in arid and semiarid regions, is soil salinization (Hanin *et al.* 2016). Increased salt accumulation imposes osmotic stress, oxidative stress, ion toxicity, and nutrient deficiency in plants, affecting nearly all aspects of their life cycle, including germination, vegetative growth, and reproductive development (Shrivastava and Kumar 2015). Fortunately, plants have developed two types of osmolytes to avoid the osmotic effects of salt stress, one of which is made up of organic osmolytes, which play an important role in osmotic adjustment. The organic osmolytes commonly found in higher plants consist of sugars and their derivatives, amino acids, and methylated tertiary N compounds (Chen and Jiang 2010). As a typical osmoprotectant, sucrose is important for maintaining cell osmotic pressure and cell membrane stability (Lee *et al.* 2013). The cFBA is a key enzyme in the sucrose biosynthetic pathway, where it catalyzes the production of FBP from triose phosphates in the cytoplasm. Transgenic potatoes were generated that express the *E. coli cFBA* gene to improve plant yield by increasing sucrose production in general; in contrast, decreased cFBPase expression of the *cFBA* gene in *A. thaliana* leads to an inhibition of sucrose synthesis (Strand *et al.* 2000). In the present study, there were no significant differences in sucrose content in leaves among the transgenic lines and control plants (Fig. 7*G*) without salinity stress, potentially because the synthesized sucrose was rapidly transported to the phloem rather than accumulating in photosynthesizing leaves (Uematsu *et al.* 2012). However, tobacco overexpressing the *AhFBA* gene might profit from more sucrose synthesized via the FBA-involved biosynthesis pathway and stored in leaves when exposed to salt stress, which could promote their water potential under salinity stress.

Proline usually accumulates in a variety of plants in response to biotic and abiotic stresses (Hayat *et al.* 2012) and it can also be used as an osmolyte to assist plants in adjusting their cellular osmotic potential. In this study, transgenic lines overexpressing the *AhFBA* gene subjected to salt stress accumulated more proline than control plants suggesting that increased proline might help plants avoid the osmotic stress induced by high salinity. In accordance with this study, there is a strong relationship between the shoot water potential of *Reaumuria vermiculata* and NaCl-enriched nutrient solutions, and also proline accumulation in transgenic tobacco shoots significantly increased with increaing NaCl exposure (Fig. 7*H*), which might play a critical role in osmoregulation.

Apart from causing osmotic stress, high salinity can also trigger the generation of reactive oxygen species (ROS), such as H_2O_2, within plant cells, which (at a high level) results in the oxidative damage of membrane lipids, sugars, proteins, and nucleic acids (AbdElgawad *et al.* 2016). To cope with the oxidative stress resulting from ROS, a complex scavenging system consisting of enzymatic and nonenzymatic antioxidants has been evolved in higher plants. In addition to acting as an osmolyte, proline can also be considered an antioxidant, which contributes to ROS scavenging (Wu *et al.* 2014). The application of exogenous proline drastically reduces the oxidative damage to lipid membranes in tobacco caused by salinity (Okuma *et al.* 2004). In the present study, control plants accumulated 2.33-fold more H_2O_2 under salt stress for 7 d. However, only a slight increase in H_2O_2 content was detected in transgenic tobacco plants (Fig. 7*C*). This observation imply that overexpression of the *AhFBA* gene either inhibited H_2O_2 generation or effectively scavenged excess H_2O_2 by proline.

In this study, the *AhFBA* gene was cloned from *A. hypogaea* and functionally characterized. Bioinformatic analysis reveals that AhFBA belonged to the class-I aldolases, and *in silico* and *in vivo* localization studies suggest that the AhFBA protein was localized in the cytoplasm. Prokaryotic expression revealed notably enhanced salinity tolerance and survival of *E. coli*. Transgenic tobacco overexpressing the *AhFBA* gene exhibited a lower H_2O_2 content, electrolyte leakage, and malondialdehyde content and a higher photosynthetic efficiency, P_N, relative water content, sucrose content, and proline content, compared to control plants. Taken together, the results indicate that overexpression of *AhFBA* increased the tolerance of *E. coli* and *N. tabacum* to salinity stress, probably by scavenging H_2O_2 and maintaining the osmotic balance.

Reference

Abd Elgawad, H., Zinta, G., Hegab, M.M., Pandey, R., Asard, H., Abuelsoud, W.: High salinity induces different oxidative stress and antioxidant responses in maize seedlings organs. - Front. Plant Sci. **7**: 1-11, 2016.

Cai, B., Li, Q., Xu, Y., Yang, L., Bi, H., Ai, X.: Genome-wide analysis of the fructose 1, 6-bisphosphate aldolase (FBA) gene family and functional characterization of FBA7 in tomato. - Plant Physiol. Biochem. **108**: 251-265, 2016.

Chen, H., Jiang, J.-G.: Osmotic adjustment and plant adaptation to environmental changes related to drought and salinity. - Environ. Rev. **18**: 309-319, 2010.

Chen, Y., Cui, J., Li, G., Yuan, M., Zhang, Z., Yuan, S., Zhang, H.: Effect of salicylic acid on the antioxidant system and photosystem II in wheat seedlings. - Biol. Plant. **60**: 139-147, 2016.

Cheng, L., Wang, Y., He, Q., Li, H., Zhang, X., Zhang, F.: Comparative proteomics illustrates the complexity of drought resistance mechanisms in two wheat (*Triticum aestivum* L.) cultivars under dehydration and rehydration. - BMC Plant Biol. **16**: 188-210, 2016.

Cieśla, M., Mierzejewska, J., Adamczyk, M., Farrants, A.-K.Ö., Boguta, M.: Fructose bisphosphate aldolase is involved in the control of RNA polymerase III-directed transcription. - BBA **1843**: 1103-1110, 2014.

Dennis, E., Gerlach, W., Walker, J., Lavin, M., Peacock, W.: Anaerobically regulated aldolase gene of maize:a chimaeric origin? - J. mol. Biol. **202**: 759-767, 1988.

Fan, W., Zhang, Z., Zhang, Y.: Cloning and molecular characterization of fructose-1,6-bisphosphate aldolase gene regulated by high-salinity and drought in *Sesuvium portulacastrum*. - Plant Cell Rep. **28**: 975-984, 2009.

Flechner, A., Gross, W., Martin, W.F., Schnarrenberger, C.: Chloroplast class I and class II aldolases are bifunctional for fructose-1, 6-biphosphate and sedoheptulose-1,7-biphosphate cleavage in the Calvin cycle. - FEBS Lett. **447**: 200-202, 1999.

Gross, W., Lenze, D., Nowitzki, U., Weiske, J., Schnarrenberger, C.: Characterization, cloning, and evolutionary history of the chloroplast and cytosolic class I aldolases of the red alga *Galdieria sulphuraria*. - Gene **230**: 7-14, 1999.

Haake, V., Zrenner, R., Sonnewald, U., Stitt, M.: A moderate decrease of plastid aldolase activity inhibits photosynthesis, alters the levels of sugars and starch, and inhibits growth of potato plants. - Plant J. **14**: 147-157, 1998.

Hanin, M., Ebel, C., Ngom, M., Laplaze, L., Masmoudi, K.: New insights on plant salt tolerance mechanisms and their potential use for breeding. - Front. Plant Sci. **7**: 1-17, 2016.

Hayat, S., Hayat, Q., Alyemeni, M.N., Wani, A.S., Pichtel, J., Ahmad, A.: Role of proline under changing environments: a review. - Plant Signal. Behav. **7**: 1456-1466, 2012.

Kagaya, Y., Nakamura, H., Ejiri, S.-i., Tsutsumi, K.-i., Hidaka, S.: The promoter from the rice nuclear gene encoding chloroplast aldolase confers mesophyll-specific and light-regulated expression in transgenic tobacco. - Mol. gen. Genet. **248**: 668-674, 1995.

Kavas, M., Akça, O.E., Akçay, U.C., Peksel, B., Eroğlu, S., Öktem, H.A., Yücel, M.: Antioxidant responses of peanut (*Arachis hypogaea* L.) seedlings to prolonged salt-induced stress. - Arch. Biol. Sci. **67**: 1303-1312, 2015.

Konishi, H., Yamane, H., Maeshima, M., Komatsu, S.: Characterization of fructose-bisphosphate aldolase regulated by gibberellin in roots of rice seedling. - Plant mol. Biol. **56**: 839-848, 2004.

Lao, X., Azuma, J.-i., Sakamoto, M.: Two cytosolic aldolases show different expression patterns during shoot elongation in moso bamboo, *Phyllostachys pubescens* Mazel. - Physiol. Plant. **149**: 422-431, 2013.

Lebherz, H., Leadbetter, M., Bradshaw, R.: Isolation and characterization of the cytosolic and chloroplast forms of spinach leaf fructose diphosphate aldolase. - J. biol. Chem. **259**: 1011-1017, 1984.

Lee, B.-R., Muneer, S., Park, S.-H., Zhang, Q., Kim, T.-H.: Ammonium-induced proline and sucrose accumulation, and their significance in antioxidative activity and osmotic adjustment. - Acta Physiol. Plant. **35**: 2655-2664, 2013.

Lv, G.Y., Guo, X.G., Xie, L.P., Xie, C.G., Zhang, X.H., Yang, Y., Xiao, L., Tang, Y.Y., Pan, X.L., Guo, A.G.: Molecular characterization, gene evolution, and expression analysis of the fructose-1,6-bisphosphate aldolase (FBA) gene family in wheat (*Triticum aestivum* L.). - Front. Plant Sci. **8**: 1-18, 2017.

Mohapatra, S., Mittra, B.: Protein glutathionylation protects wheat (*Triticum aestivum* var. Sonalika) against *Fusarium* induced oxidative stress. - Plant Physiol. Biochem. **109**: 319-325, 2016.

Okuma, E., Murakami, Y., Shimoishi, Y., Tada, M., Murata, Y.: Effects of exogenous application of proline and betaine on the growth of tobacco cultured cells under saline conditions. - Soil Sci. Plant Nutr. **50**: 1301-1305, 2004.

Páez-Valencia, J., Valencia-Mayoral, P., Sánchez-Gómez, C., Contreras-Ramos, A., Hernández-Lucas, I., Martínez-Barajas, E., Gamboa-deBuen, A.: Identification of fructose-1,6-bisphosphate aldolase cytosolic class I as an NMH7 MADS domain associated protein. - Biochem. biophys. Res. Commun. **376**: 700-705, 2008.

Park, J., Tran, L. H., Jung, S.: A protoporphyrinogen oxidase gene expression influences responses of transgenic rice to oxyfluorfen. - Biol. Plant. **61**: 659-666, 2017.

Patel, M. K., Joshi, M., Mishra, A., Jha, B.: Ectopic expression of *SbNHX1* gene in transgenic castor (*Ricinus communis* L.) enhances salt stress by modulating physiological process. - Plant Cell Tissue Organ Cult. **122**: 477-490, 2015.

Purev, M., Kim, M.K., Samdan, N., Yang, D.-C.: Isolation of a novel fructose-1,6-bisphosphate aldolase gene from *Codonopsis lanceolata* and analysis of the response of this gene to abiotic stresses. - Mol. Biol. **42**: 179-186, 2008.

Schmittgen, T.D., Livak, K.J.: Analyzing real-time PCR data by the comparative CT method. - Nat. Protoc. **3**: 1101-1108, 2008.

Shams, F., Oldfield, N.J., Wooldridge, K.G., Turner, D.P.: Fructose-1,6-bisphosphate aldolase (FBA) – a conserved glycolytic enzyme with virulence functions in bacteria: 'ill met by moonlight'. - Biochem. Soc. Trans. **42**: 1792-1795, 2014.

Shi, H., Wang, Y., Cheng, Z., Ye, T., Chan, Z.: Analysis of natural variation in bermudagrass (*Cynodon dactylon*) reveals physiological responses underlying drought tolerance. - PLoS ONE **7**: e53422, 2012.

Shrivastava, P., Kumar, R.: Soil salinity: a serious environmental issue and plant growth promoting bacteria as one of the tools for its alleviation. - Saudi J. biol. Sci. **22**: 123-131, 2015.

Singh, P.K., Shrivastava, A.K., Chatterjee, A., Pandey, S., Rai, S., Singh, S., Rai, L.: Cadmium toxicity in diazotrophic *Anabaena* spp. adjudged by hasty up-accumulation of transporter and signaling and severe down-accumulation of nitrogen metabolism proteins. - J. Proteomics **127**: 134-146, 2015.

Strand, Å., Zrenner, R., Trevanion, S., Stitt, M., Gustafsson, P., Gardeström, P.: Decreased expression of two key enzymes in the sucrose biosynthesis pathway, cytosolic fructose-1,6-bisphosphatase and sucrose phosphate synthase, has remarkably different consequences for photosynthetic carbon metabolism in transgenic *Arabidopsis thaliana*. - Plant J. **23**: 759-770, 2000.

Sui, J., Jiang, D., Zhang, D., Song, X., Wang, J., Zhao, M., Qiao, L.: The salinity responsive mechanism of a hydroxyproline-tolerant mutant of peanut based on digital gene expression profiling analysis. - PLoS ONE **11**: e0162556, 2016.

Toscano, S., Farieri, E., Ferrante, A., Romano, D.: Physiological and biochemical responses in two ornamental shrubs to drought stress. - Front. Plant Sci. **7**: **??-??**, 2016.

Uematsu, K., Suzuki, N., Iwamae, T., Inui, M., Yukawa, H.: Increased fructose 1,6-bisphosphate aldolase in plastids enhances growth and photosynthesis of tobacco plants. - J. exp. Bot. **63**: 3001-3009, 2012.

Wu, G., Wang, G., Ji, J., Gao, H., Guan, W., Wu, J., Guan, C., Wang, Y.: Cloning of a cytosolic ascorbate peroxidase gene from *Lycium chinense* Mill. and enhanced salt tolerance by overexpressing in tobacco. - Gene **543**: 85-92, 2014.

Zeng, Y., Tan, X., Zhang, L., Jiang, N., Cao, H.: Identification

and expression of fructose-1,6-bisphosphate aldolase genes and their relations to oil content in developing seeds of tea oil tree (*Camellia oleifera*). - PLoS ONE **9**: e107422, 2014.

Zeng, Y., Tan, X., Zhang, L., Long, H., Wang, B., Li, Z., Yuan, Z.: A fructose-1, 6-biphosphate aldolase gene from *Camellia oleifera*: molecular characterization and impact on salt stress tolerance. - Mol. Breed. **35**: 17, 2015.

Zhang, F., Li, S., Yang, S., Wang, L., Guo, W.: Overexpression of a cotton annexin gene, *GhAnn1*, enhances drought and salt stress tolerance in transgenic cotton. - Plant mol. Biol. **87**: 47-67, 2015.

Zhang, F., Zhang, P., Zhang, Y., Wang, S., Qu, L., Liu, X., Luo, J.: Identification of a peroxisomal-targeted aldolase involved in chlorophyll biosynthesis and sugar metabolism in rice. - Plant Sci. **250**: 205-215, 2016.